Spectrochimica Acta Part A: Molecular and Biomolecular Spectroscopy 136 (2015) 931–936

Contents lists available at ScienceDirect

Spectrochimica Acta Part A: Molecular and Biomolecular Spectroscopy

journal homepage: www.elsevier.com/locate/saa

$\chi^{(3)}$ measurement and optical power limiting behavior of manganese doped lithium tetraborate nanoparticles

R. Mohandoss [a], S. Dhanuskodi [a,*], G. Vinitha [b]

[a] School of Physics, Bharathidasan University, Tiruchirappalli 620 024, India
[b] Division of Physics, School of Advanced Sciences, V.I.T. University, Chennai 600 048, India

HIGHLIGHTS

- Nanoparticles of $Li_2B_4O_7$:Mn was synthesized following sol–gel method.
- No absorption peaks are found in the visible region of UV spectrum.
- Addition of Mn with LTB provides wide range of laser output clamping value.

GRAPHICAL ABSTRACT

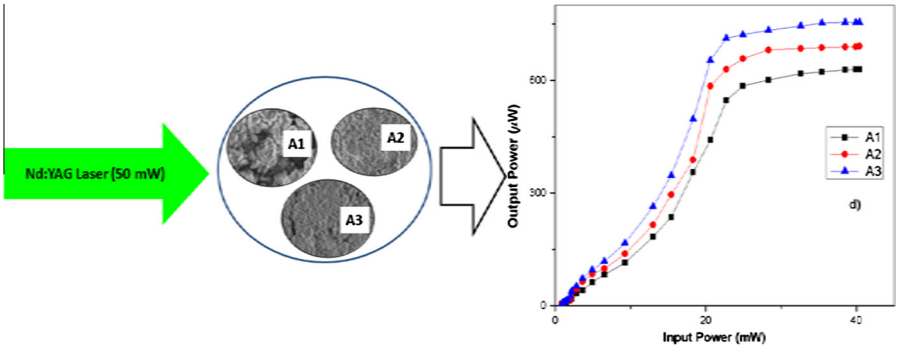

ARTICLE INFO

Article history:
Received 2 June 2014
Received in revised form 21 September 2014
Accepted 28 September 2014
Available online 5 October 2014

Keywords:
Sol–gel processing
Structural characterization
Nonlinear optics

ABSTRACT

Manganese doped $Li_2B_4O_7$ nano crystallites were prepared by chemical method and characterized by XRD, FTIR, UV and fluorescence spectra. FESEM reveals that the particles are coagulated and the particle size is in the range of 50–107 nm. Bands appear at 682–769 cm^{-1}corresponds to the bending of B–O linkage in borate network. Nonradiative energy transfer process is observed from fluorescence spectrum. UV–Vis studies show the samples are completely transparent in the visible region and having absorption peaks (234 and 276 nm) in UV regime. The measured second harmonic generation values are 0.9 times KDP. The nonlinear optical parameters such as nonlinear refractive index, n_2 (10^{-8} cm^2/W), nonlinear absorption, β (10^{-2} cm/W) and nonlinear optical susceptibility, $\chi^{(3)}$ (10^{-5} esu) are estimated using a Nd:YAG laser (532 nm, 50 mW).

Introduction

Nonlinear optical materials exhibiting nonlinear absorption are of current interest. They are used with low power lasers for applications such as phase conjugation, image processing, optical switching and to protect eye and sensors from energetic light pulses [1–3]. The laser intensity induced changes of optical transmittance at higher laser power are due to several physical mechanisms. For example, in the case of quantum electronics and laser spectroscopy, saturable absorption in atoms and molecules are observed because of the decrease in occupancy in their lower energy level [4]. Among inorganic nonlinear optical materials, borates possess unique optical properties like very low cut off wavelength (down 200 nm), high laser damage threshold (40 GW/cm^2), nuclear radiation resistance and excellent second and third order nonlinear properties ($\chi^{(2)}$, $\chi^{(3)}$) [5]. Lithium tetraborate has $[B_4O_9]^{6-}$ structural pattern consisting of two planar trigonal (BO_3) and two tetrahedral (BO_4) units with interstitial Li atom [6]. Kar et al. have hinted that the addition of Mn with $Li_2B_4O_7$ makes the compound suitable for detecting low

* Corresponding author at: School of Physics, Bharathidasan University, Tiruchirappalli 620 024, Tamil Nadu, India. Tel.: +91 0431 2407057; fax: +91 0431 2407045.
E-mail address: dhanus2k3@yahoo.com (S. Dhanuskodi).

http://dx.doi.org/10.1016/j.saa.2014.09.116
1386-1425/

dose rate radiations and possesses high thermo-luminescent efficiency [7]. Also, the improved luminescence efficiency of LTB:Mn single crystals has been observed which is twice Mg and Cu doping [8]. The present work is mainly focused on the synthesis of LTB:Mn nanoparticles with different concentrations. Low power optical limiting behavior of the undoped and doped samples was extensively studied using a diode pumped Nd:YAG laser (532 nm, 50 mW).

Experimental

Synthesis of nanocrystalline $Li_2B_4O_7$:Mn

A typical method for preparing LTB:Mn nanocrystals follows: Lithium hydroxide monohydrate was dissolved in 100 ml of double distilled water and stirred for 20 min. Manganese acetate [$(CH_3COO)_2Mn{\cdot}4H_2O$] of for different doping levels (0.01 M, 0.03 M, 0.05 M) was added and the solution appeared brownish turbid. H_3BO_3 was added to the solution and allowed to react for 30 min at 50 °C. The pH was measured as 10.25 (0.00 M), 9.17 (0.01 M) (A1), 8.77 (0.03 M) (A2) and 8.71 (0.05 M) (A3). The resultant solution was kept for gelation and the dry gel was obtained after a period of 15 days. The final product was preheated at 150 °C for 1 h in hot air oven and sintered at 500 °C for 1 h in a SiC furnace.

Instrumentation

PANalytical X'Pert Pro powder X-ray diffractometer (Cu Kα, λ = 1.5406 Å, with a step size of 0.02° and 2θ range of 10–80°) was used to analyze the structural and crystalline orientation of LTB:Mn nanoparticles. Molecular structure was confirmed by JASCO 460 plus FTIR spectrophotometer (400–4000 cm^{-1}) following KBr pellet technique. Surface morphology was observed by FESEM (Carl Zeiss). Optical absorption spectrum (Shimadzu UV–Vis 1800, 200–800 nm, 304 K) and luminescence spectra (Fluoromax4) were recorded. Second harmonic generation efficiency was measured using a Q-switched Nd:YAG Laser (1064 nm, 9 ns, 10 Hz). The third order nonlinear optical parameters such as nonlinear refractive index (n_2), nonlinear absorption coefficient (β) and nonlinear susceptibility ($\chi^{(3)}$) were determined by Z-scan technique using a diode pumped cw Nd:YAG laser (532 nm, 50 mW). The laser beam was focused by a lens of focal length 3.5 cm and the beam waist of 14.99 μm was attained. The solution was prepared for appropriate concentration and taken in a 1 mm cuvette and it was translated along the axial region of the beam across its focal region. A detailed discussion on Z-scan and optical limiting setup was given elsewhere [9].

Results and discussion

Structural and morphological analysis

Powder XRD pattern (Fig. 1) shows polycrystalline nature of the sample. Peak broadening observed from the pattern shows that the crystallite size are in nano scale. The crystalline orientation (1 1 2) was predominant and all the planes were indexed JCPDS value (79-0963). The unit cell constants of undoped and LTB:Mn are estimated (Table 1). SEM image (Fig. 2) shows the effect of doping on the size and morphology of the samples. Inclusion of manganese into the host lattice has reduced the particle size of sample A1 (50 nm), A2 (70 nm) and A3 (107 nm).

Molecular structure

Fig. 3 shows the FTIR spectrum of undoped and LTB:Mn nanoparticles sintered at 600 °C. The spectra contains two group of bands; one at 1200–1600 cm^{-1}, due to the stretching of B–O bond of the trigonal BO_3 unit and the other at 800–1200 cm^{-1} which is attributed to the tetrahedral BO_4 unit. Another band at 682–769 cm^{-1} corresponds to the bending relaxation of B–O linkage in borate network (Table 2).

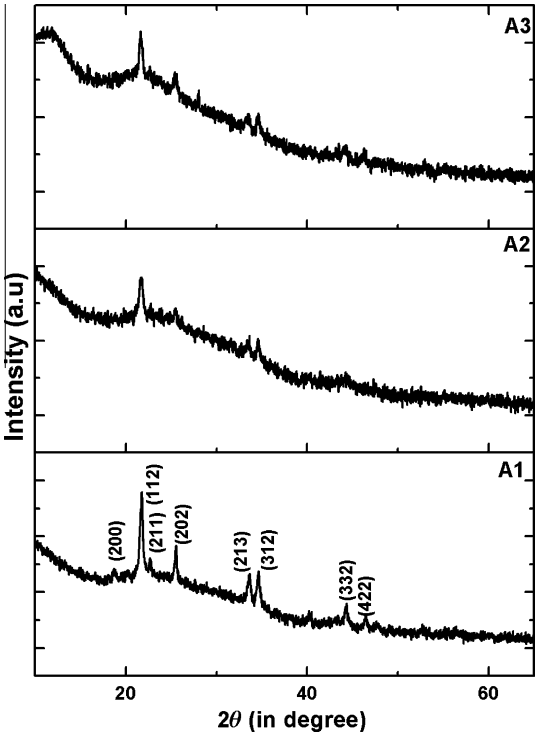

Fig. 1. Powder XRD pattern of LTB:Mn nanoparticles.

Table 1
Unit cell constants of undoped and LTB:Mn nanoparticles.

Sample	Unit cell constant (Å)	
	a	*c*
Pure LTB	9.44	10.28
Sample A1	9.47	10.28
Sample A2	9.49	10.32
Sample A3	9.46	10.43

Optical studies

UV–Vis spectrum

As a result of d–d electron transfer in the transition metal ion linked with oxygen, a week absorption at 240 nm and a shoulder at 271 nm for A1 and intense peaks at 229 and 234 nm and small hump at 283 nm and 295 nm were observed for A2 and A3 (Fig. 4). Due to the parity and spin forbidden character of d–d transition, no optical absorption band is detected in the visible region [10].

Luminescence spectrum

Fig. 5 shows the luminescence spectrum of lithium tetraborate doped with manganese. Manganese in the $3d^5$ system with a ^6S ground state is a well-known activator in many systems [11]. Absence of 307 nm emission shows that the energy transfer is non-radiative. For A2 the emission peak at 364 nm is due to the $^4T_2$ (^4D) transition, which gets suppressed for A1 and a weak emission band at 344 nm is found for A3. A shoulder at 405 and 435 nm